CrossMark

ORIGINAL PAPER

Effects of charge ratios of xylan-poly(allylamine hydrochloride) complexes on their adsorption onto different surfaces

María Verónica Galván · María Soledad Peresin · Paulina Mocchiutti ·
Niko Granqvist · Miguel Ángel Zanuttini · Tekla Tammelin

Abstract The adsorption behavior of polyelectrolyte complexes (PECs) of poly(allylamine hydrochloride) (PAH) and 4-O-methylglucuronoxylan (Xyl) onto silica surface, cellulose nanofibrils (CNFs) model surfaces, and unbleached softwood kraft fibers was studied. Different charge ratios and ionic strengths of the liquid medium (q^-/q^+: 0.3, 0.5 and 0.8 in 1 mM NaCl, and q^-/q^+: 0.2, 0.3 and 0.5 in 10 mM NaCl), at pH 7.5 were considered. First, the complexes obtained were characterized by measuring the charge density, the particle size and the zeta potential. Then, the adsorption of PAH alone and PECs on silica and CNF model surfaces were studied by quartz crystal microbalance with dissipation monitoring (QCM-D) and surface plasmon resonance (SPR). The QCM-D test indicated that: (a) adsorbed cationic layers of PECs were soft in 10 mM NaCl, (b) higher adsorption was observed at higher ionic strength and (c) the highest adsorption of complex and coupled water was

found at a charge ratio of 0.3. The SPR results analyzed together with the corresponding QCM-D results revealed that a significant portion of the adsorbed layers corresponded to coupled water on the cationic PEC structures. Morphology and structures of the adsorbed PEC layers studied using atomic force microscopy showed that the majority of the PECs were spherical, while some bigger aggregates were also found. Finally, the retention of different PECs on an unbleached softwood pulp was determined and the maximum retention was obtained when the PEC charge ratio was 0.5 in a 10 mM NaCl solution.

Keywords Ionic strength · Cellulose nanofibrils · Unbleached cellulosic fibers · QCM-D · SPR

M. V. Galván · P. Mocchiutti · M. Á. Zanuttini
Instituto de Tecnología Celulósica, Facultad de Ingeniería Química, Universidad Nacional del Litoral, Santa Fe, Argentina

M. S. Peresin (✉) · T. Tammelin
VTT Technical Research Centre of Finland, Espoo, Finland
e-mail: soledad.peresin@vtt.fi

N. Granqvist
BioNavis Ltd., Ylöjärvi, Finland

Introduction

Polyelectrolyte complexes (PECs) can be obtained by mixing solutions of oppositely charged polyelectrolytes. The major driving force behind their formation has been described in terms of electrical interactions between oppositely charged polyelectrolytes and entropy gain caused by the release of counterions (Ankerfors 2008; Chen et al. 2003; Koetz and Kosmella 2007), but inter-macromolecular hydrogen bonding, van der Waals, dipole–dipole and hydrophobic interactions can also occur (Koetz and Kosmella 2007).

PECs are attractive for many fields. They can be used in the food industry to achieve colloidal stability of the products (Gärdlund et al. 2003), and in biomedicine, as protein immobilizers and carriers for gene therapy or drug delivery (Lankalapalli and Kolapalli 2009; Saether et al. 2008). In papermaking, complexes can be used as retention aid (Petzold et al. 1996), for water treatment and flocculation (Petzold et al. 1996; Petzold and Schwarz 2014) and as dry strength additives (Gernandt et al. 2003; Gärdlund et al. 2003, 2005; Ankerfors 2008). Recently, Mocchiutti et al. (2015) showed that the addition of PECs onto high quality unbleached fibers considerably increased the papermaking properties. These complexes were based on a cationic polyelectrolyte—poly(allylamine hydrochloride) (PAH)—and one of the following anionic polyelectrolytes: a synthetic one, polyacrylic acid (PAA) or a natural one, 4-*O*-methylglucuronoxylan (Xyl).

Several factors influence the conformation of PECs, such as concentration, charge density, molecular mass, order of addition, chain flexibility of the polyelectrolytes, ionic strength and pH of the liquid medium, among others (Kabanov and Zezin 1984; Ström et al. 1985; Dautzenberg 1997; Chen et al. 2003). They can be characterized using various techniques, e.g. polyelectrolyte titration (Terayama 1952; Mocchiutti et al. 2015), turbidimetry (Ström et al.1985; Hubbe et al. 2005), zeta potential (Kramer et al. 1997; Saether et al. 2008), and atomic force microscopy (AFM) (Norgren et al. 2007; Ankerfors 2008).

Quartz crystal microbalance with dissipation monitoring (QCM-D) can be used to characterize the adsorption behavior of PECs on sensor surfaces. The technique is based on the acoustic oscillation of quartz crystal with detection limits on the range of nanograms per cm^2. Changes in frequency are related to changes in mass of the layer attached to the quartz surface, while measuring dissipation is useful to monitor changes in viscoelasticity at the interface. Surface plasmon resonance (SPR) is a very sensitive optical technique that has also been used to analyze biopolymer adsorption (Orelma et al. 2011; Eronen et al. 2011). It was employed to measure the dry adsorbed mass of polymer on a gold sensor chip. Therefore, the combined use of QCM-D and SPR techniques allows gaining a deeper understanding on the adsorption of the PECs onto the substrate surfaces.

Several authors have used silica sensor to evaluate the adsorption of polyelectrolyte multilayers films (Saarinen et al. 2008; Lingström and Wågberg 2008; Gärdlund et al. 2003), polyampholytes (Song et al. 2010) and PECs (Ankerfors 2008; Saarinen et al. 2008) on QCM-D studies. Studies on cellulose, xylan, and lignin model surfaces have been of interest in many investigations (Tammelin et al. 2006; Saarinen et al. 2008; Peresin et al. 2012; Norgren et al. 2007).

The development of cellulose nanofibrils (CNFs) allows the deposition of fibrils on silica surfaces by spin-coating. CNFs can be obtained by mechanical fibrillation of wood pulp, using refining, homogenization, or a combination of both methods (Siró and Plackett 2010). CNFs have the advantage of keeping the chemical composition and fibrillar morphology of the original pulp fibers (Ahola et al. 2008a).

This study focused on the characterization of PECs formed from PAH and xylan at different charge ratios and different ionic strengths. The mechanisms and the driving forces for the adsorption of PECs and PAH onto silica surface and cellulose nanofibrils model surface as well as the amount of PECs retained on an unbleached softwood kraft pulp, were investigated.

Materials and methods

Polyelectrolytes

Xylan

The anionic polyelectrolyte used was 4-*O*-methylglucuronoxylan (Xyl), isolated from beechwood by alkaline extraction. It was provided by Sigma-Aldrich (product number X-4252) as a powder, with an average molecular mass of M_w: 18.7 kDa, and polydispersity of 1.8 determined by Size Exclusion Chromatography (SEC). Fresh solutions of 0.9 meq/L were daily prepared in 10^{-4} N NaOH solution. Ionic strength values of 1 and 10 mM NaCl were considered. Solutions were heated in a water bath at 95 °C for 15 min to dissolve xylan, as reported by Linder et al. (2003). The pHs of the solutions were adjusted to 7.5.

Poly(allylamine hydrochloride) (PAH)

The cationic polyelectrolyte used was poly(allylamine hydrochloride) (PAH) (M_w: 56 kDa). It was also provided by Sigma-Aldrich as a powder and was used

as received to prepare a 0.23 meq/L solution at ionic strength values of 1 and 10 mM NaCl at pH 7.5.

The charge densities of PAH and xylan were reported in previous works (Galván et al. 2013; Mocchiutti et al. 2015) and are shown in Table 1.

Polyelectrolyte complex formation (PECs)

PECs were prepared at charge ratios (q^-/q^+) of 0.2, 0.3, 0.5 and 0.8, being the term charge ratio defined as the ratio between the number of charges of the polyelectrolyte in deficiency (xylan) and the number of charges of the polyelectrolyte in excess (PAH).

Complexes were formed in a Britt Dynamic Drainage Jar and using a syringe pump to add different volumes of xylan solution (0.9 meq/L) at a dosage rate of 30 mL/h on a 300 mL PAH solution (0.23 meq/L) under continuous controlled stirring (300 rpm), similarly to Mocchiutti et al. (2015). The added volumes of xylan were 22, 37 and 59 mL in 1 mM NaCl for charge ratios of 0.3, 0.5 and 0.8, respectively, and 16, 27 and 42 mL in 10 mM NaCl for charge ratios of 0.2, 0.3 and 0.5, respectively.

Characterization of the polyelectrolyte complexes

Charge densities

PEC charge densities were determined by the polyelectrolyte titration method (Terayama 1952) using a standard solution of potassium (polyvinyl sulfate) (KPVS) from AppChem as titrant. A 200 μN KPVS solution in deionized water was prepared for polyelectrolyte titrations. Before titrating, an o-toluidine blue indicator (OTB) was added to the complex solutions in 1 mM or 10 mM NaCl and the pH was adjusted to 7.5 using NaOH. The indicator color change was on-line monitored by the spectrophotometric method (Mocchiutti and Zanuttini 2007).

Table 1 Polyelectrolyte charge densities at different ionic strengths at pH 7.5

Polyelectrolyte	Charge densities (meq/g)[a]	
	1 mM NaCl	10 mM NaCl
PAH	+9.90 ± 0.10	+8.29 ± 0.03
Xylan	−0.86 ± 0.02	−0.96 ± 0.04

[a] The standard deviations of the means from two replicates of the trial are indicated

Z-potential and particle size measurements

Polyelectrolyte complexes with different charge ratios and different ionic strengths of the liquid medium at pH 7.5 were analyzed using a Zetasizer Nano Series (Malvern Instruments, United Kingdom). The measurements of size and z-potential were performed at 25 °C. A refractive index close to the one of water should be chosen because PEC particle contains a lot of water (Cegnar and Ker 2010).

Streaming current measurements

PEC formations were monitored through streaming current measurements using Chemtrac ECA 2100 equipment (USA). Titrations were performed by adding a xylan solution at a dosage rate of 30 mL/h on a PAH solution at the corresponding ionic strength (1 mM NaCl or 10 mM NaCl), and pH 7.5. The value of zero in the streaming current signal was considered as an indicator of the neutralization of polyelectrolyte charges.

Preparation of cellulose nanofibrils (CNFs) and CNF model surface

Preparation of CNFs

Industrial liner paper (100 % virgin softwood fibers from *Pinus elliottii* and *Pinus taeda*) supplied by Papel Misionero S.A. (Argentina) was mechanically processed using a Masuko grinder (three times) followed by disintegration in a fluidizer (Microfluidics Int, CO, USA), 20 passes. The resulting CNF suspension had a consistency of 1.6 wt%. It was sonicated and then centrifuged at 8800 rpm for 2 h. Colloidal nanofibrils were then collected from supernatant. The content of total acid groups of the CNFs was 38 ± 2 μeq/g. This content was determined by the conductometric method using 0.1 N NaHCO$_3$ (Katz et al. 1984; NaHCO$_3$ was used instead of NaOH according to Lloyd and Horne 1993).

Preparation of CNF model surface

CNF model surfaces were prepared using a high shear spin coating method (WS400BNPP Spincoater- Laurell Technologies Corporation, PA, USA). SiO$_2$-crystals substrates were first cleaned using UV/

ozonator (BioForce Nanoscience UV/O$_3$ Procleaner™ Ames, IA, USA) for 10 min, followed by immersion into a 10 mg/mL aqueous polyvinyl amide (anchoring polymer) solution for 30 min, followed by rinsing with milliQ-water (Ahola et al. 2008b) and drying with nitrogen. Then, 35 μL of water were spin-coated on the SiO$_2$-crystal surfaces (15 s, 3000 rpm), followed by 50 μL of the supernatant nanofibrils suspension (at 3000 rpm for 45 s). Finally, the sensors were rinsed with MilliQ-water, dried with nitrogen and placed in an oven for 1 h at 80 °C to evaporate the remaining water and fix the CNF film on the substrate, prior to the QCM-D and SPR runs.

Quartz crystal microbalance with dissipation monitoring (QCM-D) measurements

Quartz crystal microbalance with dissipation monitoring QCM-D E4 (Q-Sense AB, Gothenburg, Sweden) was used to studied the adsorption of PAH and polyelectrolyte complexes on silica surface and on CNF model surfaces. QCM-D allows the simultaneous monitoring of changes on frequency and dissipation as a function of time when the sensors are exposed to PECs flow. Changes on frequency and dissipation can be interpreted in terms of mass adsorbed and structural changes in the adsorbed layer, respectively.

The fundamental frequency (f_0) used was 5 MHz. All the data were processed with the QTools software and its overtones (15, 25, 35 and 45 MHz) were used to determine the masses adsorbed of the viscoelastic complexes. The data were fitted to the Voigt viscoelastic model. The following parameters were considered: the fluid density (1000 kg/m^3), fluid viscosity (0.001 kg/ms) and film density (1200 kg/m^3).

Different complex charge ratios and only PAH at different ionic strengths of the liquid medium (q^-/q^+: 0, 0.3; 0.5 and 0.8 in 1 mM NaCl, and q^-/q^+: 0, 0.2; 0.3 and 0.5 in 10 mM NaCl) were considered. First, a stable baseline was obtained at the corresponding ionic strength, and then the adsorptions of PAH and the polyelectrolyte complexes were monitored. The experiments were made at pH 7.5 and PECs were diluted to 50 mg/L prior to the QCM-D runs. The solutions under continuous stirring were passed through the sensor chambers at a flow rate of 100 μL/min for 30 min and at 23 °C. Then, the surfaces were rinsed with salt solutions in order to remove loosely bound material. At the end of each

QCM-D run, MilliQ-water was circulated through the chamber. The sensors were finally dried with N$_2$ and placed in a desiccator in order to keep the surface free from contamination for further morphological analysis by AFM. Two replicas were made for each condition.

Surface plasmon resonance (SPR)

The SPR experiments were employed to analyze adsorption of complexes on silica sensors using a SPR Navi 200 (Oy BioNavis Ltd., Ylöjärvi, Finland). SPR was used to measure the dry adsorbed mass of complexes. The adsorption of an adsorbate to the surface of the SPR sensor can be monitored in real time if the adsorbate has a different refractive index from that of the bulk solution (Jung et al. 1998). Changes in either refractive index or layer thickness on the SPR sensor alter the specific SPR angle (Sambles et al. 1991; Jung et al. 1998; Malmström et al. 2013).

The thickness of adsorbed layers of complexes, d, was determined by Eq. (1) (Jung et al. 1998):

$$d = \frac{l_d}{2} \frac{\Delta_{angle}}{m(n_a - n_0)} \tag{1}$$

where the Δ_{angle} is a change in the SPR angle in °, the $l_d/2$ is a characteristic evanescent electromagnetic field decay length (240 nm) and estimated as 0.37 of the light wavelength, m is a sensitivity factor for the sensor (109.94°/RIU), n_0 is the refractive index of the bulk solution (1.334 RIU), and n_a is the refractive index of the adsorbed polyelectrolyte. In this work, the refractive index was assumed to be 1.5 RIU for PECs (Granqvist et al. 2013). The surface excess concentration (Γ) was calculated according to Eq. (2):

$$\Gamma = d \cdot p \tag{2}$$

where d is the calculated thickness of the adsorbed layer in nm, and ρ is the specific volume of an adsorbate (1.2 g/cm^3).

All the experiments were performed at a constant flow rate of 100 μL/min, considering different charge ratios (q^-/q^+: 0.2, 0.3 and 0.5) at an ionic strength of 10 mM NaCl at pH 7.5. Adsorptions of the complexes were performed on silica surfaces and on CNF model surfaces. The CNF films were equilibrated overnight in MilliQ-water. The SPR measurements were stabilized using a 10 mM NaCl solution for 10 min and then, the complex solutions were injected until a

constant ΔSPR angle was obtained. Finally, surfaces were rinsed with 10 mM NaCl solution for 40 min. All experiments were made in duplicate.

Atomic force microscopy (AFM)

Images of the silica surface and CNF model surface used for the QCM-D study were analyzed by using a Nanoscope IIIa Multimode scanning probe microscope (Digital Instruments Inc. Santa Barbara, CA, USA). The images were scanned using tapping mode with silicon cantilevers with a nominal resonance frequency of 320–360 kHz, supplied by μMasch (Tallin, Estonia). No image processing was performed except flattening.

Pulp preparation

Industrial liner paper (100 % virgin softwood fibers from *P. elliottii* and *P. taeda*) supplied by Papel Misionero S.A. (Argentina) was cut in sheets and soaked for 12 h in water. Then, following the procedure described in Mocchiutti et al. (2015), the sheets were repulped, classified (collecting the R100 fraction), acidified up to pH 4.0, and stored until use.

The chemical characteristics of the pulp used in this work were previously reported in Galván et al. (2013). Particularly, the surface acid groups were 21.0 ± 0.5 μeq/g pulp, the total charge was 90.6 ± 0.2 μeq/g pulp and total lignin was 12.65 ± 0.04 % on the original pulp.

PEC retention curves

Wet samples of 0.55 g of o.d. pulp were added to 360 mL complex suspensions of different concentrations, at different charge ratios (q^-/q^+: 0.2, 0.3 and 0.5), in 10 mM NaCl of ionic strength at pH 7.5, while being continuously stirred using a Britt Dynamic Drainage Jar similar to Mocchiutti et al. (2015). The amount of complexes in the filtrate was indirectly determined by measuring the amount of xylan in the initial and filtered solutions by means of the phenol–sulphuric acid method (Hodge and Hofreiter 1962). As reported by Hubbe et al. (2005), a test was performed in order to determine the amount of soluble and fine material (*S/F*) and the amount of complex retained was calculated according to Eq. (3):

Amount of complex retained

$$= \frac{\left(PEC_I - PEC - \frac{S}{F}\right)\text{mg}}{g_{pulp}} \quad (3)$$

where PEC_I is the amount of initial complex added on pulp, mg; *PEC*, the amount of complex on the filtrate, mg; *S/F*, the amount of soluble and fines released from the pulp determined in the absence of complex, mg; and g_{pulp}, the dry mass of pulp, g.

Results and discussion

Characterization of polyelectrolyte complexes

Charge densities of the complexes

Table 2 shows the charge densities of the Xyl/PAH complexes prepared at different charge ratios and different ionic strengths (q^-/q^+: 0.3, 0.5 and 0.8 in 1 mM NaCl solution, and q^-/q^+: 0.2, 0.3 and 0.5 in 10 mM NaCl solution). As expected, the charge densities of the PECs decrease when the complex charge ratio is increases, i.e. when more xylan was added for complex preparation. Nevertheless, the experimental values obtained were significantly lower than the theoretical ones, particularly when the complexes were prepared in 1 mM NaCl solution. This behavior indicates deviations from the 1:1 stoichiometry during complex preparation, as

Table 2 Charge densities of complexes determined by polyelectrolyte titration at pH 7.5 and different charge ratios and ionic strengths

Different charge ratios q^-/q^+	Charge densities of complexes (meq/g)[a]		
	Theoretical values	Experimental values	
		1 mM NaCl	10 mM NaCl
0.2	+1.90	n.d	+1.44 ± 0.01
0.3	+1.20	+0.17 ± 0.01	+0.37 ± 0.01
0.5	+0.55	–	+0.06 ± 0.02
0.8	+0.14	−1.02 ± 0.06	n.d.

Complex charge ratios were calculated taken into account the charge densities of the polyelectrolytes PAH and xylan (Table 1)

[a] The standard deviations of the means from two replicates of the trial are indicated. For a charge ratio of 0.5 and 1 mM NaCl, the charge density could not be determined. *n.d.* not determined

previously reported by others (Chen et al. 2003; Mocchiutti et al. 2015). In these cases, a fraction of the PAH cationic charge is not accessible for the anionic polyelectrolyte on titration and remains with their corresponding counterions in the PEC structure.

Table 2 also shows that for 1 mM NaCl solution, when the PEC charge ratio was 0.8, the experimental charge density was negative, while when it was 0.5, the charge density could not be determined probably because the charge value was too low (near zero) to be detected using the polyelectrolyte titration method.

Z-potential and streaming potential measurements

Figure 1a shows z-potential results as a function of the PEC charge ratio. At higher ionic strength, z-potential values were always positive, while at lower ionic

strength, a negative z-potential value was obtained for the PECs charge ratio of 0.8. When the charge ratio was 0.5, for both ionic strengths, the z-potential was close to zero. These results are in agreement with the experimental charge densities shown in Table 2.

Figure 1b shows streaming current results as a function of PEC charge ratios for the same two ionic strengths. The figure also shows that the streaming current signal is strongly reduced when the ionic strength of the liquid medium is increased. The amount of titrant corresponding to the zero streaming current signal is increased with increasing salt concentration. Both results are similar to those found by Chen et al. (2003) using potassium (polyvinyl sulfate) (KPVS) and poly-diallyldimethylammonium chloride (polyDADMAC) at different salt concentrations.

Although these two techniques have different working principles, results of z-potential and streaming current measurements exhibited similar trends. Both techniques showed: (a) values are always positive at 10 mM NaCl and (b) the PEC electrical charge is negative when the charge ratio is 0.8 at 1 mM NaCl.

Size measurements

Table 3 shows the sizes of Xyl/PAH complexes determined by Zetasizer at two ionic strengths. The results show that the higher the PEC charge ratio, the larger the size of the complexes. For a charge ratio of 0.2 and 0.3, the majority of the complexes (95.6–99.3 %) were between 190 and 339 nm in size,

Table 3 Size of the polyelectrolyte complexes at different charge ratios, pH 7.5 and two ionic strengths

Different charge ratios q^-/q^+	Size (nm)	
	1 mM NaCl	10 mM NaCl
0.2	n.d.	190 ± 0.4 (97.5 %)
		4953 ± 119 (2.5 %)
0.3	339 ± 0.3 (99.3 %)	320 ± 7 (95.6 %)
	4832 ± 120 (0.7 %)	4955 ± 139 (4.4 %)
0.5	–	–
0.8	441 ± 20 (84.3 %)	n.d
	4759 ± 617 (15.7 %)	

The standard deviations of the means from two replicates of the trial are shown. For a charge ratio of 0.5, the particle size could not be determined. *n.d.* not determined
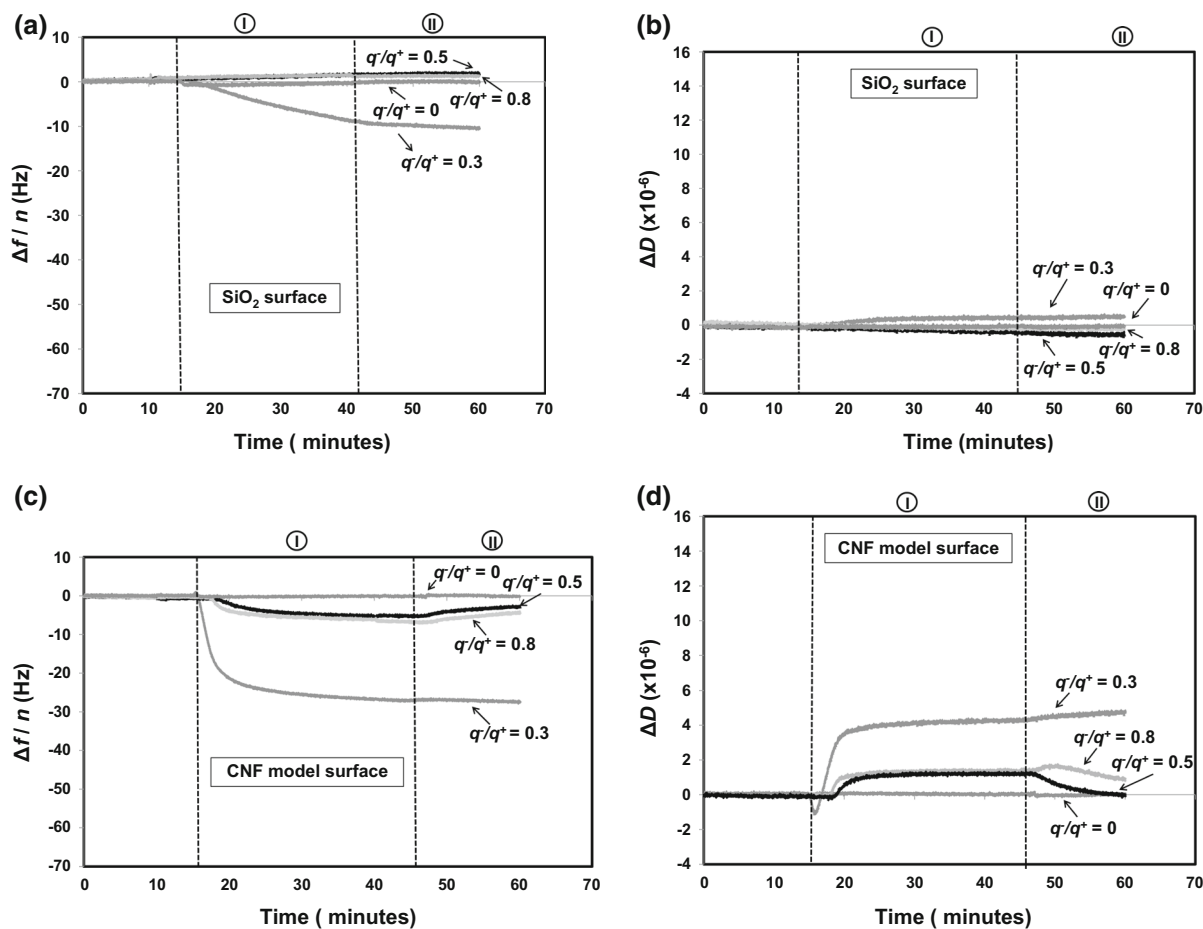
Fig. 1 Z-potential of complexes determined by Zetasizer (**a**) and streaming current signal measured by Chemtrac equipment during the complex formation (**b**) as a function of different charge ratios (q^-/q^+: 0, 0.2, 0.3, 0.5 and 0.8) and salt concentrations (1 and 10 mM NaCl). Complexes were prepared by adding xylan solution on PAH solution. Charge ratio q^-/q^+: 0 corresponds to original PAH solution

Fig. 2 Change in frequency (**a**, **c**) and dissipation (**b**, **d**) as a function of time for adsorption of complexes on silica surface and CNF model surfaces at different charge ratios (q^-/q^+: 0, 0.2, 0.3 and 0.5), and salt concentration: 1 mM NaCl, monitored by

QCM-D ($f_0 = 5$ MHz, overtone number n = 3). *I* PEC adsorption, *II* Rinse with NaCl 1 mM. The PEC concentrations were 50 ppm. A charge ratio q^-/q^+: 0 corresponds to original PAH solution

while a low percentage (0.7–4.4 %) showed a larger size (approximately 4900 nm). Nevertheless, for charge ratio of 0.8, a higher amount of large size complexes (15.7 %) was found.

For charge ratios of 0.5 and at both ionic strengths, the particle size could not be determined because the Zetasizer equipment is unable to measure size when the charge of the complexes is very close to neutrality, as shown in Table 2 and Fig. 1.

In order to facilitate the interpretation of the adsorption behavior of the polyelectrolyte complexes formed by slightly anionic xylan and clearly cationic PAH on highly charged anionic silica or on CNF surface with moderate anionic charge, the essential previously reported features and the findings of this study are collected as follows.

PECs with distinct charges show moderate stability (z-potential varying from ±30 to ±40 mV) or incipient instability in solution (z-potential varying from ±10 to ±30 mV), see Fig. 1. They form colloidal, non-soluble complexes since already at low addition levels of xylan yields turbid solutions (Mocchiutti et al. 2015). Theoretical PEC charge density values are larger than the experimental values (Table 2) indicating non-stoichiometric relationship (Mocchiutti et al. 2015; Chen et al. 2003) where non-specific electrostatic interactions are taking place (Ström et al. 1985).

Cationic PEC with the charge ratio of 0.3 in 1 mM NaCl is moderately stable colloid with rather uniform size distribution (particle size ∼340 nm) and high streaming current signal (Fig. 1; Table 3). This
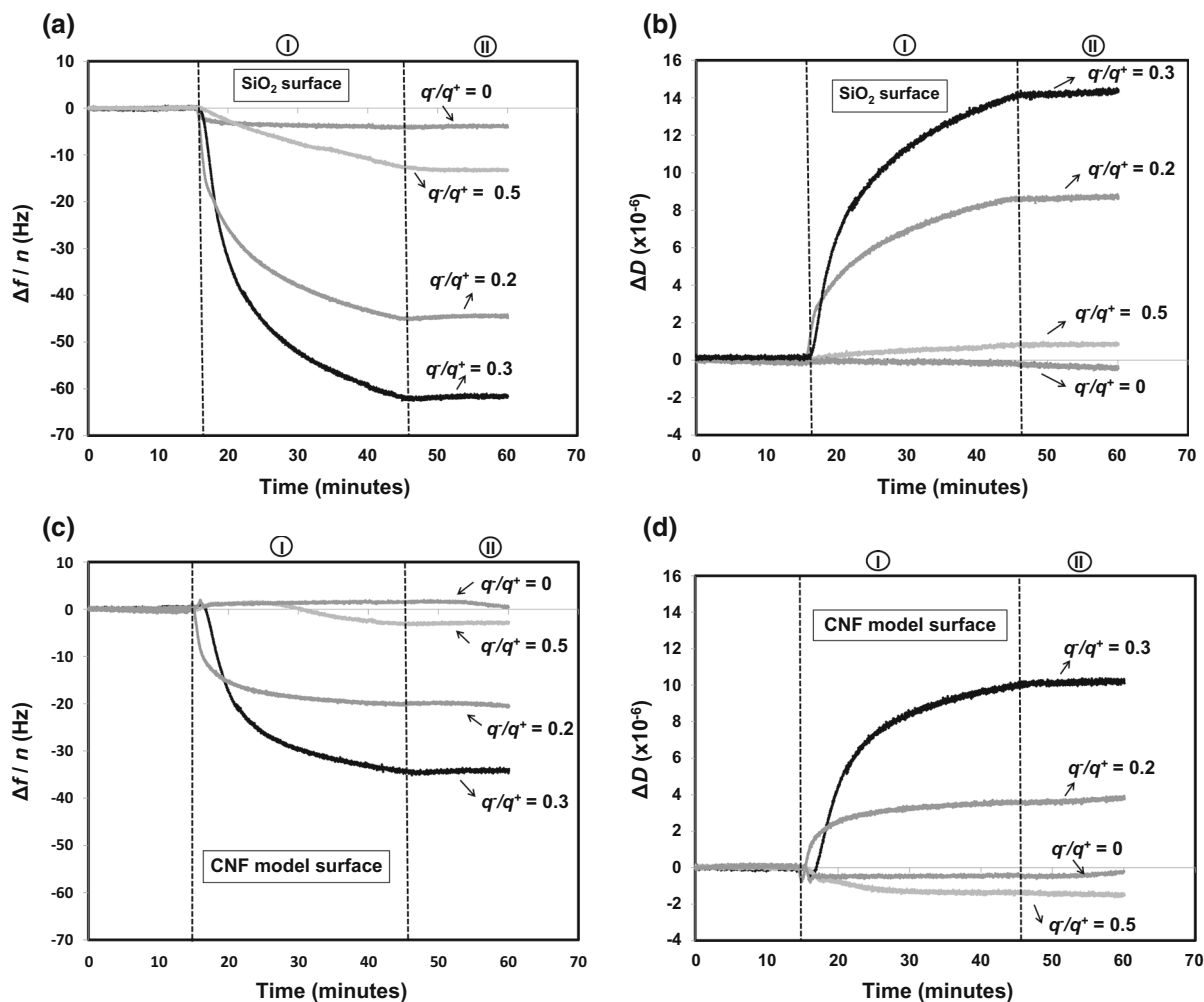
Fig. 3 Change in frequency (**a**, **c**) and dissipation (**b**, **d**) as a function of time for adsorption of complexes on silica surface and CNF model surfaces at different charge ratio (q^-/q^+: 0, 0.3, 0.5 and 0.8) and salt concentration: 10 mM NaCl monitored by

QCM-D ($f_0 = 5$ MHz, overtone number n $= 3$). *I* PEC adsorption, *II* Rinse with NaCl 10 mM. The PEC concentrations were 50 ppm. A charge ratio q^-/q^+: 0 corresponds to original PAH solution

particular complex shows the highest stability in solution studied in this paper.

Cationic PECs with the charge ratios of 0.2 and 0.3 in 10 mM NaCl can be regarded as systems with incipient instability (zeta potential $\sim$ 10–30 mV). It has been shown that the addition of small amounts of NaCl lowers the agglomeration tendency and the radius of gyration of the complexes increase with increasing salt concentration (Dautzenberg and Jaeger 2002; Dautzenberg 1997). Therefore, these colloidal PECs are still stable within the timescale and conditions utilized here but small changes in solution

properties, e.g. further increase in ionic strength may induce severe flocculation.

At charge ratio of 0.5 with both electrolyte concentrations, the PECs are close to the charge neutralization. This leads to highly unstable system seen as complex phase separation and precipitation. Charge densities and size of the PECs were unreasonable to analyse due to neutral net charge and severe flocculation.

At charge ratio of 0.8 in 1 mM NaCl, the charge of the PEC was clearly anionic. The system possessed weak stability with the tendency to easily flocculate.

Adsorption of PECs on SiO_2 and on CNF model surfaces at different ionic strengths monitored by QCM-D

Adsorption from 1 mM NaCl

Figure 2a, c shows the changes in frequency as a function of time when pure cationic PAH or complexes formed by xylan and PAH with different charge ratios are adsorbed on highly anionic silica surface and on cellulose nanofibril (CNF) model surface from 1 mM NaCl concentration, respectively. Figure 2b, d shows the simultaneously recorded changes in dissipation values as a function of time. After replacement of 1 mM NaCl solution in the QCM-D cell with a solution of PAH or Xyl/PAH complex, the adsorption equilibrium was generally attained within 30 min.

When adsorbing pure cationic PAH $(q^-/q^+ = 0)$ on highly anionic silica the frequency change is very small and the change in dissipation is only slightly above the detection limit. Thus, the adsorbed layer of PAH is thin and rigidly attached to the oppositely charged surface. This is in good agreement with the previous findings of the similar kind of systems with charged cationic starch (Tammelin et al. 2004) and pDADMAC (Saarinen et al. 2008) adsorbed on silica where the electrostatic repulsion expands the polyelectrolyte coil and only a small amount of polyelectrolyte is needed to neutralise the anionic surface charges.

The adsorption behaviour seems to be similar towards less anionic CNF surface. If any adsorption takes place the surface is instantaneously covered by very thin PAH layer. However, the existence of the PAH layer on CNF is uncertain since other methods were not utilised to confirm this assumption.

As shown by the Fig. 2a, b, none of the Xyl/PAH complexes has specific attractive affinity towards silica. In the cationic system $(q^-/q^+ = 0.3)$, some adsorption can be detected but both frequency and dissipation change values are so minor that more preferably some free polyelectrolyte molecules are adsorbed and swiftly occupying the anionic surface preventing the true complex adsorption to take place (Ondaral et al. 2010). Notably, higher frequency and dissipation changes should be expected during the significant adsorption of polyelectrolyte complexes, see Saarinen et al. (2008). At the charge ratio of 0.5 Xyl/PAH, complexes show severe precipitation due to

charge neutralisation and therefore the conditions do not favour the adsorption behaviour whereas at the charge ratio of 0.8, the complexes are anionic, generating the electrostatic repulsion between complexes and the anionic surface which hinders the adsorption to occur.

On CNF surface the complex adsorption behaviour is similar except now, the cationic complex $(q^-/q^+ = 0.3)$ seems to adsorb to somewhat higher extent, see Fig. 2c, d. This is probably due to the attractive forces not only within cationic groups onto anionic CNF but also due to specific attractive interactions within xylan and cellulosic structures as also
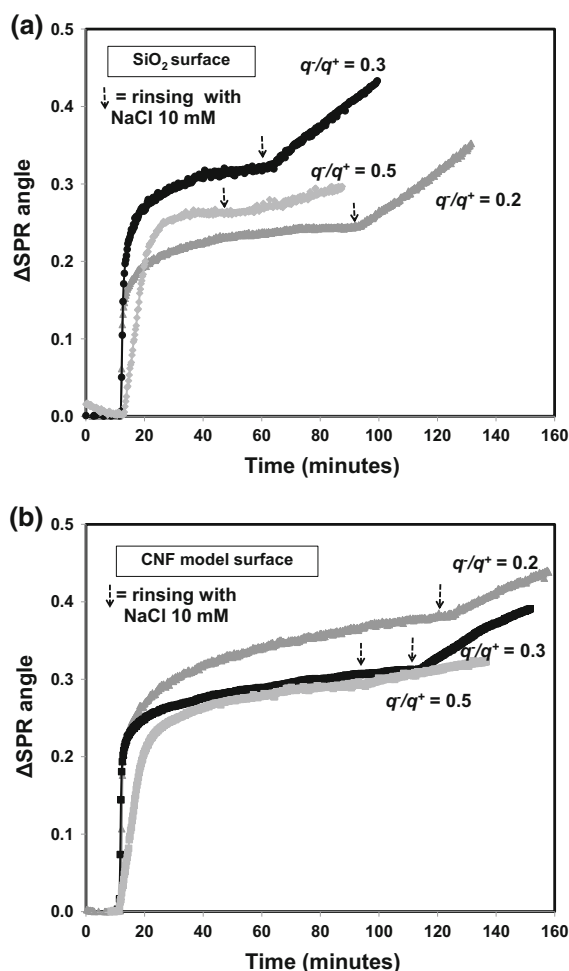

Fig. 4 SPR sensograms for the adsorption of polyelectrolyte complexes on silica surface (**a**) and CNF model surface (**b**) at different charge ratios: q^-/q^+: 0.2, 0.3 and 0.5. Medium condition: 10 mM NaCl at pH: 7.5. The PEC concentrations were 50 ppm

previously shown (Tammelin et al. 2009; Eronen et al. 2011).

Adsorption from 10 mM NaCl

Figure 3a, c shows the changes in frequency as a function of time when pure cationic PAH or complexes formed by xylan and PAH with different charge ratios are adsorbed on highly anionic silica surface and on moderately anionic cellulose nanofibril (CNF) model surface from 10 mM NaCl concentration, respectively. Figure 3b, d show the simultaneously recorded changes in dissipation values as a function of time. After replacement of 10 mM NaCl salt solution in the QCM-D cell with a solution of PAH or Xyl/PAH complex, the adsorption equilibrium was generally attained within 30 min.

The most interesting results were achieved with cationic PECs with the charge ratios (q^-/q^+) of 0.2 and 0.3. Slight increase in ionic strength (1 mM NaCl → 10 mM NaCl) clearly increase the adsorbed amount and now Xyl/PAH complexes with cationic charge evidently adsorb on both silica and on CNF surfaces as shown in Fig. 3a, c. Simultaneously, the adsorbed amount increases as the charge density of the complex is decreasing. This behavior is typical for high charged PECs and it is well in accordance with the previous findings (Ankerfors and Wågberg 2014). Such adsorption behavior, which is not a result of the pure electrosorption only, has been explained with the build-up of an osmotic pressure due to non-neutralized charges of the adsorbed complexes. It has been suggested that the structure of the colloidal complexes is a charged, almost spherical coil with the neutral core and charged outer surface with associated counter ions. The amount of charges associated with one complex is more than enough to recharge the area of

Fig. 5 Topographic AFM images of (a) silica, (b) Xyl/PAH▶ complexes at charge ratios of 0.2, (c) 0.3 adsorbed on silica and (d) 0.5 precipitation on silica; Ionic strength: 10 mM NaCl. Ra: is the roughness average. The image size is 2×2 µm
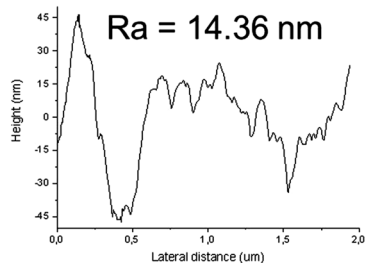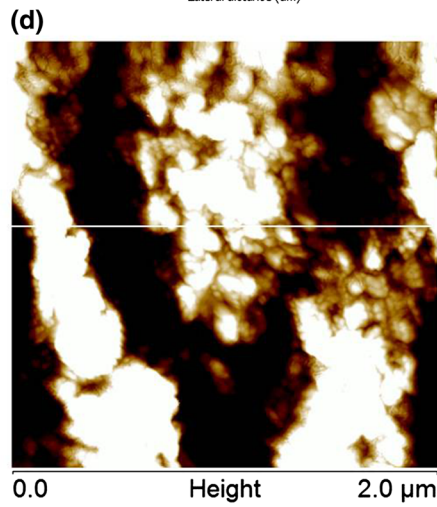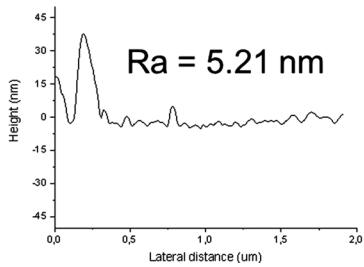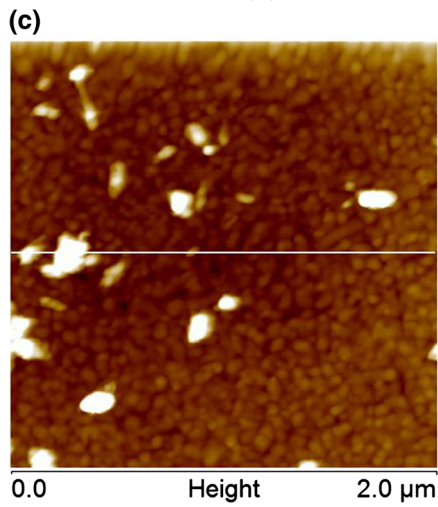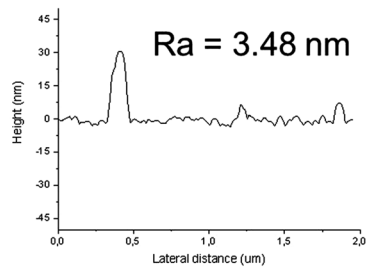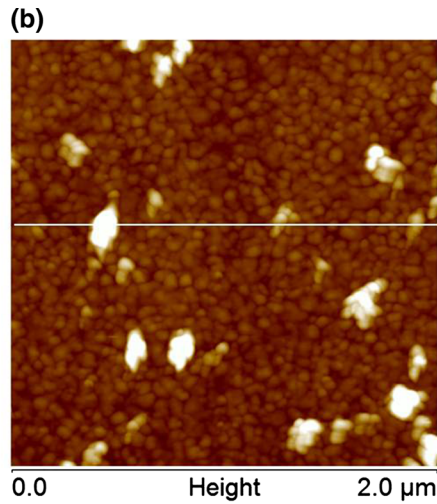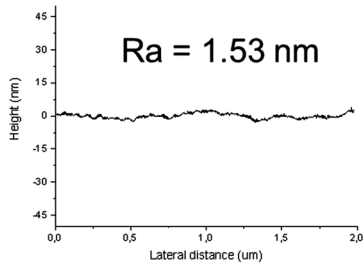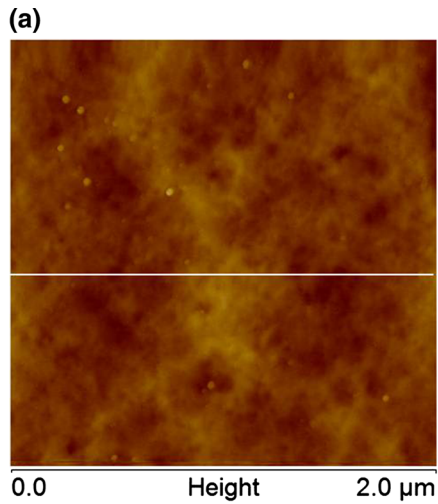
the solid surface occupied by the adsorbed PEC, i.e. the amount of counter ions released from the complexes will not be the same as the amount released from the solid surface. Therefore, the surface will be recharged which leads to a build-up of an osmotic pressure which prevents further PECs to adsorb. Increase in electrolyte concentration will decrease the osmotic pressure upon PEC adsorption which results in an increased adsorbed amount of PEC. The other reason for the behavior could be that, the increase in the ionic strength of the medium promotes conformational changes on the polyelectrolyte complexes. The charges of polyelectrolytes are screened with increasing electrolyte concentration (van de Ven 2000) and this increases the flexibility of the polyelectrolytes, thus allowing easier access to the ionic groups on the surface (Horvath et al. 2006). As shown by the Table 3, the size of the PEC ($q^-/q^+ = 0.3$) is slightly reduced when the ionic strength is increased, probably due to more compact conformation at higher ionic strength. Van de Stegg et al. (1992) found that the screening-enhanced polyelectrolyte adsorption regime appears when both non-electrostatic and electrostatic interactions are introduced.

The highest adsorbed amount of PECs and water was obtained when a charge ratio of 0.3 was used, which corresponds to PECs with a slightly cationic charge density. Saarinen et al. (2008) found similar results when complexes of anionic and cationic polyacrylamides (A-PAM/C-PAM) with charges near to neutrality, but still being slightly cationic, were adsorbed on silica and on cellulose surface.
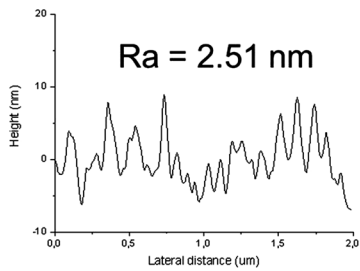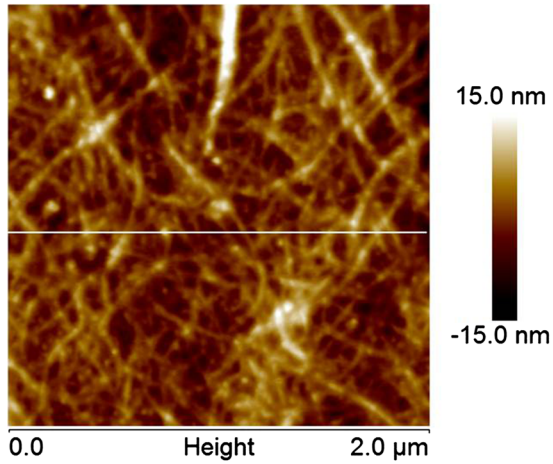
Table 4 Mass and % water content of layer of Xyl/PAH complexes adsorbed on silica surface and on CNF model surface determined by QCM-D and SPR

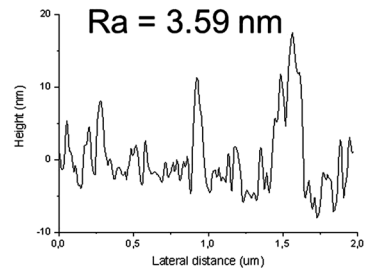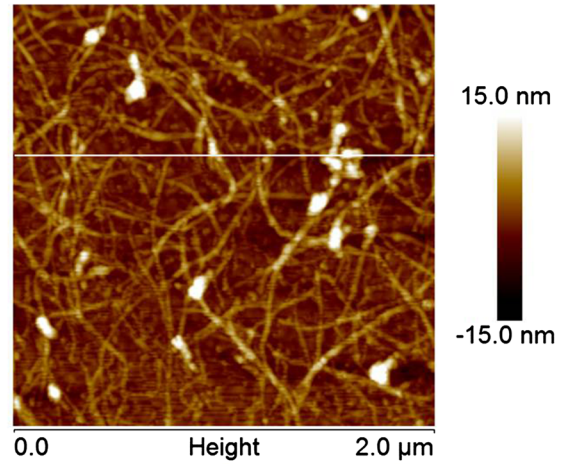| Surface	Different charge ratios q^-/q^+	Δm_{QCM-D} (mg/m^2)	Δm_{SPR} (mg/m^2)	% coupled water
Silica	0.2	55.6 ± 0.3	3.0 ± 0.1	95
	0.3	60.2 ± 1.1	3.8 ± 0.1	94
	0.5	3.3 ± 0.6	3.5 ± 0.4	–
CNF	0.2	54.1 ± 1.1	4.4 ± 0.2	92
	0.3	88.2 ± 1.2	3.5 ± 0.4	96
	0.5	0.6 ± 0.4	3.7 ± 0.2	–

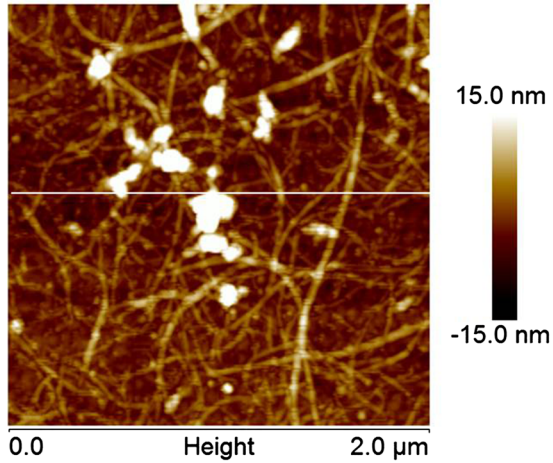The standard deviations of the means from two replicates of the trial are shown

(a)

15.0 nm

−15.0 nm

0.0   Height   2.0 µm

Ra = 2.51 nm

(b)

15.0 nm

−15.0 nm

0.0   Height   2.0 µm

Ra = 3.59 nm

(c)

15.0 nm

−15.0 nm

0.0   Height   2.0 µm

Ra = 3.92 nm

(d)

15.0 nm

−15.0 nm

0.0   Height   2.0 µm
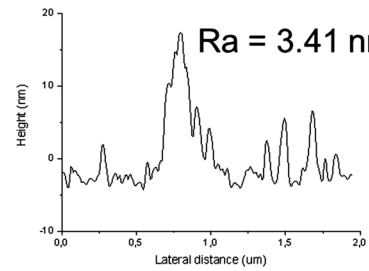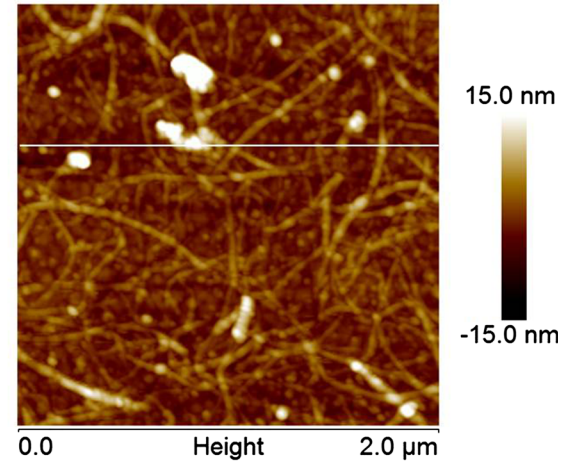
Ra = 3.41 nm
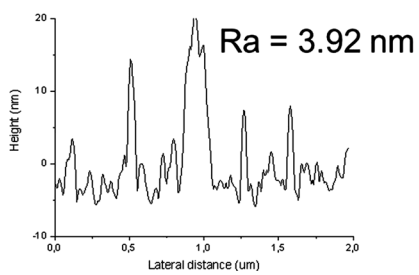
◀ **Fig. 6** Topographic AFM images of (**a**) cellulose nanofibrils, (**b**) Xyl/PAH complexes at charge ratios of 0.2, (**c**) 0.3 and (**d**) 0.5 adsorbed on cellulose nanofibrils. Ionic strength: 10 mM NaCl. Ra: is the roughness average. The image size is 2 × 2 μm
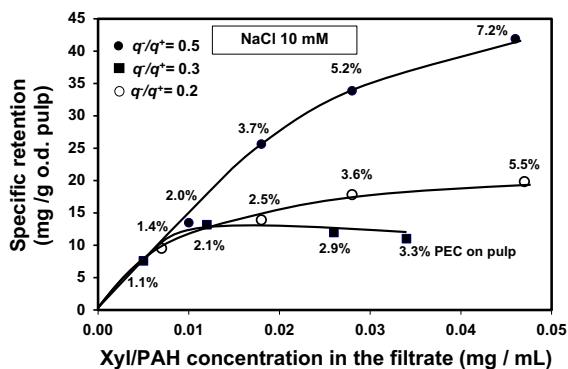

Fig. 7 Specific retention of Xyl/PAH complexes as a function of the PEC concentrations in the filtrate, at different charge ratios (q^-/q^+: 0.2, 0.3 and 0.5). Medium conditions: 10 mM NaCl at pH 7.5

Figure 3b, d shows significant changes in dissipation as a function of time when cationic PECs with the charge ratio of 0.2 and 0.3 were adsorbed on silica surface and on CNF model surface, respectively. The clear changes in dissipation indicate that the adsorbed layers are soft, more mobile and water rich when adsorbed on solid surface with anionic charge.

PEC with the charge ratio of 0.5 shows severe precipitation due to the charge neutralisation and therefore, the interpretation of the QCM-D data with respect to true complex adsorption behaviour is not meaningful.

Finally, it can be noted that the adsorption of PECs on the CNF model surface followed the same trends as shown on silica surface, see Fig. 3c, d. Furthermore, the results clearly show that the amount of polyelectrolyte complexes adsorbed on silica was higher than on the cellulose nanofibril surface. At a given pH, the silica surface presents a higher surface charge than cellulose surfaces (Kontturi et al. 2008). It has been reported that the distance between anionic charges in the case of pure cellulose surfaces is 20 nm, while the distance is about one order of magnitude lower in the case of silica (0.2–0.3 nm) at neutral pH (Kontturi et al. 2008; Tadros and Lyklema 1968). Although the true charge density of CNF surface can be expected to be higher due to presence of acidic side groups of

hemicelluloses, the CNF anionic charge is notably lower compared to that of silica surface. This could explain the higher amount of PECs adsorbed on silica surface.

Surface plasmon resonance (SPR)

Figure 4 illustrates the adsorption of PECs on silica surface and CNF model surface monitored by SPR, at different charge ratios and ionic strength of 10 mM NaCl. Results show that a maximum adsorption of PECs can be observed at a charge ratio of 0.3 on silica surface and 0.2 on CNF model surface. Additionally, in all determinations, an increase of the ΔSPR angle after rinsing with 10 mM NaCl solution was observed. This may be caused by conformational changes of PECs adsorbed on surfaces upon rinsing (Malmström et al. 2013).

Table 4 shows the mass adsorbed and percent water content of the layer of PECs on surfaces determined by QCM-D and SPR. The masses of complexes determined by QCM-D were found to be significantly higher than the ones obtained from SPR measurements. This difference is related to water coupling on the PEC structures, indicating that the PECs structures are highly hydrated.

Morphology

Figure 5 shows the topography AFM images of silica surface and complexes of Xyl/PAH (prepared at different charge ratios and in 10 mM NaCl solution) adsorbed on silica surface. When PECs with charge ratios of 0.2 and 0.3 were adsorbed, spherical shape of the PECs and a uniform layer with few aggregates were observed (Fig. 5b, c). The average diameters of the PECs obtained from 120 measurements were 60.44 ± 7.5 and 63.75 ± 7.1 nm at charge ratios of 0.2 and 0.3, respectively. Since in this case, measurements were performed on dried complexes, their sizes were lower than the corresponding sizes measured by Zetasizer (Table 3). Complex films completely covered the silica surface and the topography was moderately smooth when there were no aggregates present. However, at a charge ratio of 0.5 (Fig. 5d), a larger amount of aggregates and a high roughness average (Ra) were observed. This can be ascribed to the low charge of the complexes, which induce to coagulation or flocculation.

Figure 6 shows the AFM images of cellulose nanofibrils adsorbed on quartz crystals coated with silica surface and complexes (prepared at different charge ratios and in 10 mM NaCl solution) adsorbed on CNF surface. Figure 6a shows that the CNFs completely covered the silica surface. Figure 6b–d also shows that the complexes with different charge ratios adsorbed on this surface are also spherical and aggregates can also be observed.

PEC retention curves

Figure 7 shows the specific retention of Xyl/PAH complexes onto cellulosic pulp as a function of the PEC concentrations in the filtrate. An ionic strength of 10 mM NaCl was considered. The amount of complex retained was indirectly determined based on Eq. (3) and using the phenol–sulphuric acid method. The retention levels of PECs on pulp were similar for charge ratios of 0.2 and 0.3, being slightly higher for the former. This is in agreement with the results of the SPR analysis, which showed the dry mass per unit of surface area adsorbed on the CNF model surface.

The highest retention was observed at a charge ratio of 0.5. This behavior could be ascribed to the larger amount of aggregates present in this case (Fig. 5d), which can be more easily retained by the pulp. This result differs with the QCM and SPR results, probably because these instruments consider a sum of several interactions such as electrical, as well as van der Walls; hydrophobic and dipole–dipole.

Conclusions

The polyelectrolyte charge ratio had a significant effect on electric charge, morphology and adsorption behavior of the Xyl/PAH complexes.

According to the QCM-D results, for both surfaces studied (silica and CNF) at low ionic strength (1 mM NaCl), the amount of complex adsorbed was low. The adsorption was clearly increased when ionic strength was increased to 10 mM NaCl. The highest amount of complex adsorbed was obtained for a Xyl/PAH charge ratio of 0.3. At this ratio, the charge density of the complex is only slightly cationic.

Taking into account the QCM-D and SPR results, the layers of complexes adsorbed were viscoelastic

and a significant portion of them corresponded to coupled water on the PEC structures.

For a Xyl/PAH charge ratios of 0.2 and 0.3, AFM images showed spherical cationic complexes forming a uniform adsorption surface with few aggregates. These complexes in solution can be considered as systems with incipient instability. Differently, PECs with a charge ratio of 0.5 that showed a charge density close to zero, are highly instable and thus, a larger amount of aggregates could be observed when they were adsorbed.

The maximum retention of complexes on cellulosic pulp was obtained for a Xyl/PAH charge ratio of 0.5 at 10 mM NaCl solution. This behavior could be due to the higher size of the complexes formed under these conditions.

References

Ahola S, Österberg M, Laine J (2008a) Cellulose nanofibrils adsorption with poly(amideamine) epichlorohydrin studied by QCM-D and application as a paper strength additive. Cellulose 15:303–314. doi:10.1007/s10570-007-9167-3

Ahola S, Salmi J, Johansson LS, Laine J, Österberg M (2008b) Model films from native cellulose nanofibrils. Preparation, swelling, and surface interactions. Biomacromolecules 9(4):1273–1282

Ankerfors C (2008) Polyelectrolyte complexes: their preparation, adsorption behaviour, and effect on paper properties. Licenciate Thesis, KTH, Department of Fibre and Polymer Technology; Stockholm, Sweden

Ankerfors C, Wågberg L (2014) Polyelectrolyte complexes for tailoring of wood fibre surfaces. Adv Polym Sci 256:1–24

Cegnar M, Ker J (2010) Self-assembled polyelectrolyte nanocomplexes of alginate, chitosan and ovalbumin. Acta Chim Slov 57:431–441

Chen J, Heitmann JA, Hubbe MA (2003) Dependency of polyelectrolyte complex stoichiometry on the order of addition. 1. Effect of salt concentration during streaming current titrations with strong poly-acid and poly-base. Colloids Surf A Physcochem Eng Asp 223:215–230

Dautzenberg H (1997) Polyelectrolyte complex formation in highly aggregating systems. 1. Effect of salt:

polyelectrolyte complex formation in the presence of NaCl. Macromolecules 30:7810–7815

Dautzenberg H, Jaeger W (2002) Effect of charge density on the formation and salt stability of polyelectrolyte complexes. Macromol Chem Phys 203(14):2095–2102

Eronen P, Österberg M, Heikkinen S, Tenkanen M, Laine J (2011) Interactions of structurally different hemicelluloses with nanofibrillar cellulose. Carbohydr Polym 86:1281–1290

Galván MV, Mocchiutti P, Schnell CN, Liitiä T, Zanuttini MA (2013) Dual-adsorption of poly(allylamine hydrochloride) and lignosulfonate onto recycled cellulosic fibers. Cellul Chem Technol 47(7–8):631–641

Gärdlund L, Wågberg L, Gernandt R (2003) Polyelectrolyte complexes for surface modification of wood fibers. II. Influence of complexes on wet and dry strength of paper. Colloids Surf A Physicochem Eng Asp 218:137–149

Gärdlund L, Forsström J, Wågberg L (2005) Influence of polyelectrolyte complexes on the strength properties of papers from unbleached kraft pulps with different yields. Nord Pulp Pap Res J 20:36–42

Gernandt R, Wågberg L, Gärdlund L, Dautzenberg H (2003) Polyelectrolyte complexes for surface modification of wood fibres I. Preparation and characterisation of complexes for dry and wet strength improvement of paper. Colloids Surf A Physicochem Eng Asp 213:15–25

Granqvist N, Liang H, Laurila T, Sadowski J, Yliperttula M, Viitala T (2013) Characterizing ultrathin and thick organic layers by surface plasmon resonance three-wavelength and waveguide mode analysis. Langmuir 29:8561–8571

Hodge JE, Hofreiter BT (1962) Determination of reducing sugars and carbohydrates. In: Whistler RL, Wolfrom ML (eds) Methods in carbohydrate chemistry. Academic Press, New York

Horvath AE, Lindstrom T, Laine J (2006) On the indirect polyelectrolyte titration of cellulosic fibers. Conditions for charge stoichiometry and comparison with ESCA. Langmuir 22(2):824–830. doi:10.1021/la052217i

Hubbe MA, Moore SM, Lee SY (2005) Effects of charge ratios and cationic polymer nature on polyelectrolyte complex deposition onto cellulose. Ind Eng Chem Res 44:3068–3074

Jung SJ, Campbell CT, Chinowsky TM, Mar MN, Yee SS (1998) Quantitative interpretation of the response of surface plasmon resonance sensors to adsorbed films. Langmuir 14(19):5636–5648. doi:10.1021/la971228b

Kabanov VA, Zezin BA (1984) Soluble interpolymeric complexes as a new class of synthetic polyelectrolytes. Pure Appl Chem 56(3):343–354

Katz S, Beatson RP, Scallan AM (1984) The determination of strong and weak acidic groups in sulfite pulps. Svensk Papperstidning 87:48–53

Koetz J, Kosmella S (2007) Polyelectrolyte and nanoparticles. Springer, Berlin

Kontturi KS, Tammelin T, Johansson L-S, Stenius P (2008) Adsorption of cationic starch on cellulose studied by QCM-D. Langmuir 24:4743–4749. doi:10.1021/la703604j

Kramer G, Buchhammer H-M, Lunkwitz K (1997) Surface modification by polyelectrolyte complexes: influence of different polyelectrolyte components and substrates. Colloids Surf A 122:1–12

Lankalapalli S, Kolapalli VRL (2009) Polyelectrolyte complexes: a review of their applicability in drug delivery technology. Indian J Pharm Sci 71(5):481–487

Linder A, Bergman R, Bodin A, Gatenholm P (2003) Mechanism of assembly of xylan onto cellulose surface. Langmuir 19:5072–5077. doi:10.1021/la0341355

Lingström R, Wågberg L (2008) Polyelectrolyte multilayers on wood fibers: influence of molecular weight on layer properties and mechanical properties of papers from treated fibers. J Colloid Interface Sci 328:233–242. doi:10.1016/j.jcis.2008.08.065

Lloyd JA, Horne CW (1993) The determination of fibre charge and acidic groups of radiata pine pulps. Nord Pulp Pap Res J 8(1):48–57

Malmström J, Nieuwoudt MK, Strover LT, Hackett A, Laita O, Brimble MA, Williams D, Travas-Sejdic J (2013) Grafting from poly(3,4-ethylenedioxythiophene): a simple route to versatile electrically addressable surfaces. Macromolecules 46(12):4955–4965. doi:10.1021/ma400803j

Mocchiutti P, Zanuttini MA (2007) Key considerations in the determination of polyelectrolyte concentration by the colloidal titration method. Bioresources 2(3):399–407

Mocchiutti P, Galván MV, Peresin MS, Schnell CN, Zanuttini MA (2015) Complexes of xylan and synthetic polyelectrolytes. Characterization and adsorption onto high quality unbleached fibers. Carbohydr Polym 116:131–139

Norgren M, Gärdlund L, Notley SM, Htun M, Wågberg L (2007) Smooth model surfaces from lignin derivates. II. Adsorption of polyelectrolytes and PECs monitored by QCM-D. Langmuir 23:3737–3743

Ondaral S, Ankerfors C, Wågberg L, Ödberg L (2010) Surface induced rearrangement of polyelectrolyte complexes: influence of complex composition on adsorbed layer properties. Langmuir 26(18):14606–14614

Orelma H, Filpponen I, Johansson L-S, Laine J, Rojas OJ (2011) Modification of cellulose films by adsorption of CMC and chitosan for controlled of biomolecules. Biomacromolecules 12:4311–4318

Peresin MS, Kammiovirta K, Harri S, Tammelin T (2012) Structure features and water interactions of etherified xylan thin films. J Polym Environ 20:895–904

Petzold G, Schwarz S (2014) Polyelectrolyte complexes in flocculation applications. Adv Polym Sci 256:25–66. doi:10.1007/12_2012_205

Petzold G, Buchhammer HM, Lunkwitz K (1996) The use of oppositely charged polyelectrolytes as flocculants and retention aids. Colloids Surf A Physicochem Eng Asp 119(1):87–92

Saarinen T, Österberg M, Laine J (2008) Adsorption of polyelectrolyte multilayers and complexes on silica and cellulose surfaces studied by QCM-D. Colloids Surf A Physcochem Eng Asp 330:134–142

Saether HV, Holme HK, Maurstad G, Smidsrod O, Stokke BT (2008) Polyelectrolyte complex formation using alginate and chitosan. Carbohydr Polym 74:813–821

Sambles JR, Bradbery GW, Yang F (1991) Optical excitation of surface plasmons: an introduction. Contemp Phys 32(3):173–183

Siró I, Plackett D (2010) Microfibrillated cellulose and new nanocomposite materials: a review. Cellulose 17:459–494

Song J, Yamaguchi T, Silva DJ, Hubbe M, Rojas O (2010) Effect of charge asymmetry on adsorption and phase separation of polyampholytes on silica and cellulose surfaces. J Phys Chem B 114:719–727

Ström G, Barla P, Stenius P (1985) The formation of polyelectrolyte complexes between pine xylan and cationic polymers. Colloids Surf 13:193–207

Tadros ThF, Lyklema JJ (1968) Adsorption of potential-determining ions at the silica-aqueous electrolyte interface and the role of some cations. J Electroanal Chem Interfacial Electrochem 17(3–4):267–275

Tammelin T, Meta J, Johansson L-S, Stenius P (2004) Viscoelastic properties of cationic starch adsorbed on quartz studied by QCM-D. Langmuir 20:10900–10909

Tammelin T, Saarinen T, Österberg M, Laine J (2006) Preparation of Langmuir–Blodgett-cellulose surfaces by using horizontal dipping procedure. Application for polyelectrolyte adsorption studies performed with QCM-D. Cellulose 13:519

Tammelin T, Paananen A, Österberg M (2009) The nanoscience and technology of renewable biomaterials. In: Lucia AL, Rojas OJ (eds) Wiley-Blackwell Publishing Ltd, West Sussex, pp 149–172

Terayama H (1952) Method of colloid titration a new titration between polymer adsorption. Colloids Surf A Physicochem Eng Asp 116:269–275

Van de Steeg HGM, Cohen Stuart MA, de Keizer A, Bijsterbosch BH (1992) Polyelectrolyte adsorption: a subtle balance of force. Langmuir 8(10):2538–2546

van de Ven TGM (2000) A model for the adsorption of polyelectrolytes on pulp fibers: relation between fiber structure and polyelectrolyte properties. Nord Pulp Pap Res J 15(5):494–501